PONTIFICIA UNIVERSIDAD CATÓLICA DEL PERÚ

ESCUELA DE POSGRADO

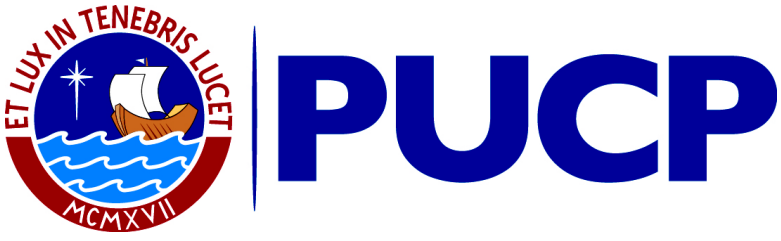

Surface tension driven flow on a thin reaction front

Tesis para optar el grado de Magíster en Física que presenta

ROBERTO ANTONIO GUZMAN RAMIREZ

Dirigido por

DESIDERIO VASQUEZ

JURADO

QUIROZ GONZALEZ, JORGE LUIS MARTIN

VASQUEZ RODRIGUEZ, DESIDERIO

VILELA PROAÑO, PABLO MARTIN

San Miguel, 2017

Eur. Phys. J. Special Topics

DOI: 10.1140/epjst/e2016-60026-4

THE EUROPEAN PHYSICAL JOURNAL SPECIAL TOPICS

Regular Article

Surface tension driven flow on a thin reaction front

Roberto Guzman[1], and Desiderio A. Vasquez[1,2,a]

[1] Departamento de Ciencias, Sección Física, Pontificia Universidad Católica del Perú Av. Universitaria 1801, San Miguel, Lima 32, Perú
[2] Department of Physics, Indiana University Purdue University Fort Wayne, Fort Wayne, IN 46805, USA

Received 11 February 2016 / Received in final form 7 June 2016
Published online xx xxx 2016

Abstract. Surface tension driven convection affects the propagation of chemical reaction fronts in liquids. The changes in surface tension across the front generate this type of convection. The resulting fluid motion increases the speed and changes the shape of fronts as observed in the iodate-arsenous acid reaction. We calculate these effects using a thin front approximation, where the reaction front is modeled by an abrupt discontinuity between reacted and unreacted substances. We analyze the propagation of reaction fronts of small curvature. In this case the front propagation equation becomes the deterministic Kardar-Parisi-Zhang (KPZ) equation with the addition of fluid flow. These results are compared to calculations based on a set of reaction-diffusion-convection equations.

1 Introduction

Chemical waves and reaction fronts propagating in liquids interact with fluid motion modifying the speed and shape of the fronts. Fluid motion can be generated by density gradients across the front due to changes in composition or thermal expansion due to heat released in the reaction. It can also be generated by changes in surface tension resulting in convective flow near the reaction front (Marangoni flow). Experiments in the Belousov-Zhabotinsky (BZ) reaction showed the presence of fluid motion induced by surface tension associated with the propagation of traveling chemical waves in an aqueous solution [1]. The motion of an aqueous droplet of the oscillatory BZ reaction on a oil phase is attributed to oscillatory changes in its surface tension [2,3]. Surface tension also explains the observation of accelerating chemical waves in the BZ reaction [4]. Experiments in the iodate-arsenous acid (IAA) reaction in open liquid layers have shown that the reaction front is elongated near the surface of the layer, an effect caused by the decrease of surface tension due to the reaction [5]. In thin reaction layers, the effects of Marangoni convection are noticed by comparing the front propagation with open and closed layers, showing that the effects of Marangoni convection are of the same order as the density driven convection [6]. Theoretical

[a] e-mail: dvasquez@pucp.edu.pe

modeling of the reaction front including surface tension convection used a reaction-diffusion equation with cubic autocatalysis to describe the front propagation [7]. The front is distorted due to changes in surface tension, with the direction of deformation depending on the sign of the surface tension gradient. In both cases, there is a speed increase due to convection. Further modeling included the effects of layer thickness [8], density gradients due concentration gradients [9], and the effects of thermal gradients due to the exothermicity of the reaction [10]. In the present work, we will use a front propagation model (instead of a reaction-diffusion equation) where the reactives and products are separated by a thin interface. This model was used sucessfully to study density driven convection in the iodate-arsenous acid reaction with good results when compared to experiments in cylinders [11,12]. This thin front evolution model can be applied to other reactions, requiring only the diffusion coefficient and the front speed, without the specific reaction term. We will model the flow using the Navier-Stokes equations in the limit of large viscosity to diffusivity ratio (Stokes flow) which corresponds to the experimental parameters of the IAA reaction [13]. We compare this results with the ones obtained using the reaction-diffusion equation.

2 Equations of motion

We consider a front propagating inside a liquid layer in two dimensions. Fluid motion obeys the incompressible Navier-Stokes equations

$$\frac{\partial \boldsymbol{V}}{\partial t} + (\boldsymbol{V}\cdot\nabla)\boldsymbol{V} = -\frac{1}{\rho_0}\nabla P + \nu\nabla^2\boldsymbol{V} - \frac{\rho}{\rho_0}g\hat{z}. \tag{1}$$

In this equation $\boldsymbol{V}$ corresponds to the fluid velocity field, P is the local pressure, ν is the kinematic viscosity, ρ is the density of the reacted solution, ρ_0 is the density of the unreacted solution, g is the magnitude of the acceleration of gravity, and $\hat{z}$ is a unit vector pointing in the vertical z direction. The fluid flow has to obey mass conservation as expressed by the continuity equation in the incompressible limit

$$\nabla\cdot\boldsymbol{V} = 0. \tag{2}$$

In this work we study the propagation of reaction fronts that separate an interface between reacted and unreacted fluids. We obtain our front evolution equation from an eikonal relation [14] between the flat front speed (c_0), the normal speed (c_n) and the curvature of the front (κ), that is: $c_n = c_0 + D\kappa$. Here D is the diffusion coefficient of the corresponding chemical. Defining a front height function $H(z,t)$ in a reference frame moving with the flat front speed, we can use the eikonal relation for small curvatures to obtain a front evolution equation under the effects of a fluid velocity field ($\boldsymbol{V}$) [16]:

$$\frac{\partial H}{\partial t} = D\frac{\partial^2 H}{\partial z^2} + \frac{c_0}{2}\left(\frac{\partial H}{\partial z}\right)^2 + V_x \tag{3}$$

which corresponds to the deterministic Kardar-Parisi-Zhang (KPZ) or Burgers equation with the addition of fluid velocity. We will also solve the reaction-diffusion-convection model with cubic autocatalysis as described in [7] to compare with the solutions of the thin front model.

We introduce dimensionless units of time and space, choosing our length scale as $L = D/c_0$ and the time scale as $\tau = D/c_0^2$. Therefore the thin front equations in these dimensionless units becomes

$$\frac{\partial H}{\partial t} = \frac{\partial^2 H}{\partial z^2} + \frac{1}{2}\left(\frac{\partial H}{\partial z}\right)^2 + V_x \tag{4}$$

A corresponding reaction-diffusion model [7] involves a coefficient of molecular diffusivity D and a concentration of a substance c that undergoes an autocatalytic reaction from an unreacted state ($c = 0$) to a reacted state ($c = 1$)

$$\frac{\partial c}{\partial t} = D\nabla^2 c + 2\alpha c^2(1-c). \tag{5}$$

This equation has a flat front solution with velocity $c_0 = \sqrt{D\alpha/2}$. We use this velocity in our definition of dimensionless units, thus the reaction-diffusion-convection system including the fluid velocity field ($\mathbf{V}$) becomes

$$\frac{\partial c}{\partial t} + \boldsymbol{V}\cdot\nabla c = \nabla^2 c + 2c^2(1-c). \tag{6}$$

In this system of units the front has a speed equal to 1.

Introducing a reduced pressure $P_r = P + \rho g z$ and neglecting density changes with the concentration ($\rho_0 = \rho$), we find a dimensionless Navier-Stokes equations using the length and time scales as above, with the reduced pressure measured in units of $\rho\nu/\tau$

$$\frac{\partial \boldsymbol{V}}{\partial t} + (\boldsymbol{V}\cdot\nabla)\boldsymbol{V} = S_c(-\nabla P_r + \nabla^2\boldsymbol{V}) \tag{7}$$

Here $S_c = \nu/D$ corresponds to the Schmidt number. We will consider only the case of infinite Schmidt number, which provides a good approximation to experimental values for the molecular diffusion and viscosity of aqueous solutions. The continuity equation Eq. (2) indicates that we can introduce a stream function ψ to obtain the fluid velocity with components $V_x = \partial\psi/\partial z$ and $V_z = -\partial\psi/\partial x$, therefore the Navier-Stokes equations can be written in terms of the stream function and the vorticity ω

$$\nabla^2\omega = 0 \tag{8}$$

and

$$\nabla^2\psi = \omega. \tag{9}$$

We will assume free boundaries in the bottom of the domain, since our main purpose is to compare our results with the ones from the reaction-diffusion model. This type of boundary conditions allows us to find an analytic solution that can be used in our numerical calculations. Free boundary conditions require zero normal fluid velocity, and that the tangential shear stress vanish, leading to a vanishing vorticity. For the lateral sides of the domain, we choose free boundary conditions located far away from the propagating front. At the top surface we require that the normal fluid velocity vanishes, which is achieved by setting the stream function equal to zero. We also impose the surface tension boundary condition for the horizontal component of the velocity

$$\mu\frac{\partial V_x}{\partial z} = \frac{\partial\gamma}{\partial x} \tag{10}$$

where γ corresponds to the surface tension, and μ is the coefficient of dynamic viscosity ($\mu = \nu\rho$). Using a linear dependence of the surface tension with the chemical concentration, we have in dimensionless units

$$\omega = -\mathrm{Ma}\frac{\partial c}{\partial x} \tag{11}$$

where $\mathrm{Ma} = -(d\gamma/dx)/(\mu\sqrt{D\alpha})$ is the dimensionless Marangoni number. The negative sign indicates that the surface tension increases with decreasing concentration c for positive Marangoni numbers as defined in [7].

3 Numerical methods

We solve the reaction-diffusion-convection Eq. (6) using a long rectangular grid, replacing the spatial derivatives by their corresponding finite difference approximations. The time evolution is carried out using a simple Euler method, where the concentrations after a time step are calculated from the equations defining the time derivatives explicitly [17]. We chose the values of grid size in dimensionless units as $\Delta x = 0.5$, $\Delta z = 0.25$, and the time step $\Delta t = 5 \times 10^{-4}$. The domain size is chosen as a rectangular box of 400 x 10 units. The evolution of the concentrations changes the boundary condition Eq. (11), we then use a relaxation method to obtain the values of the stream function and vorticity [15].

In the case of the front evolution equation Eq. (4) we also use finite difference approximations for the spatial derivatives with grid size equal to $\Delta x = 0.075$ and $\Delta z = 0.0125$. For the time evolution, we use an Euler method, where the discretize diffusive term is calculated implicitly, thus requiring the solution of a tridiagonal matrix. This allows us to use a time step equal to $\Delta t = 1.0 \times 10^{-4}$ units. We apply the method of separation of variables to obtain an analytical series solution for the Laplace equation Eq. (8) involving free boundaries at the bottom wall. We consider that the front makes contact with the upper wall at $x = 0$. Since the concentration at the front makes an abrupt jump, the boundary condition Eq. (11) includes a term proportional to a delta function. The domain is unbounded in the x direction, while the layer thickness in the z direction is represented by L_z. Using the series solution in the limit of infinite length the vorticity becomes

$$\omega(x,z) = -\frac{\mathrm{Ma}}{2L_z} \frac{\sin(\pi z/L_z)}{\cos(\pi z/L_z) + \cosh(\pi x/L_z)}. \tag{12}$$

We use the relaxation method to obtain the stream function from the vorticity solving Eq. (9). Since the vorticity-stream function equations are a set of linear equations the results are proportional to the Marangoni number, therefore we need to solve them only once. Once the stream function is obtained, we use a finite difference approach to calculate the derivatives of Eq. (4), with the time evolution provided by a simple Euler approach. Here we use a partition of 2000 points for a tube width L_z to obtain the spatial derivatives of the front height $H(z,t)$. We use an interpolation scheme to account for the velocity V_x at the position of the front.

4 Results

We show the increase of speed as a function of Marangoni number using the model based on the KPZ equation in Fig. 1. In this figure we also display our solutions for the reaction-diffusion-convection equations showing a comparable increase of speed. Here the depth of the layer thickness is kept constant at $L_z = 10$. The fronts are of constant shape moving with constant speed. For both positive and negative Marangoni numbers, the propagating fronts always show an increase of speed compared to the speed of a convectionless front. In both models positive Marangoni numbers provide a larger increase in speed compared to negative Marangoni numbers of the same absolute value. Surface tension driven convection always enhances the front speed as shown in both models. As we increase the Maragoni number, the KPZ model provides larger speeds. The gap in speed increase between both models is smaller for negative Maragoni numbers.

The shape of the front changes due to the fluid flow generated by the gradient in surface tension. The distorsion increases for larger absolute values of the Marangoni

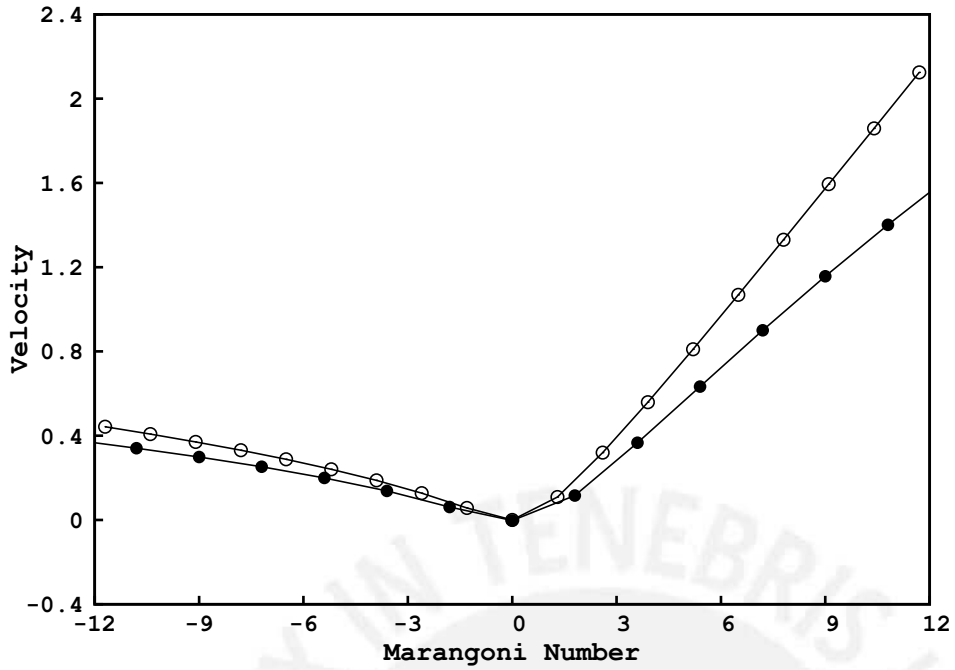

Fig. 1. The increase of front speed as a function of Marangoni number for fronts propagating on a layer of thickness $L_z = 10$. The open circles correspond to fronts described with the deterministic KPZ equation, while the solid circles are results using a reaction-diffusion equation. In both cases the speed of increase is enhanced by fluid flow.

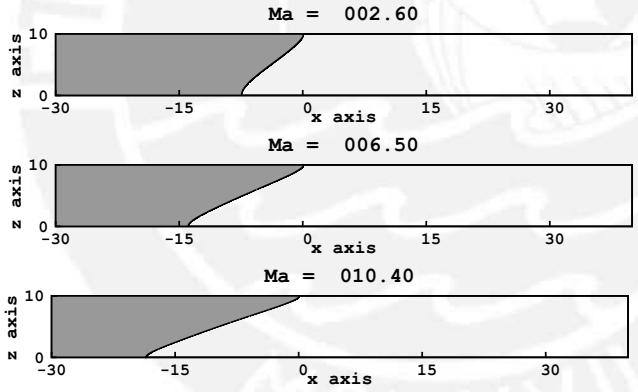

Fig. 2. Reaction fronts propagating in a fluid layer with surface tension gradients corresponding to positive Marangoni. The shape of the front develops a tip near the layer surface. The tip of the front is larger for larger Marangoni numbers.

number. Without a surface tension gradient the front would be a flat front perpendicular to the direction of propagation. We observe that in the case of positive Marangoni numbers the segment in contact with the open surface leads the front as shown in Fig. 2. Near the bottom of the container, a portion of the front lags behind as the front progates with constant speed. The distance between the tip of the front and the lagging part increases with increasing positive Marangoni number, thus the front

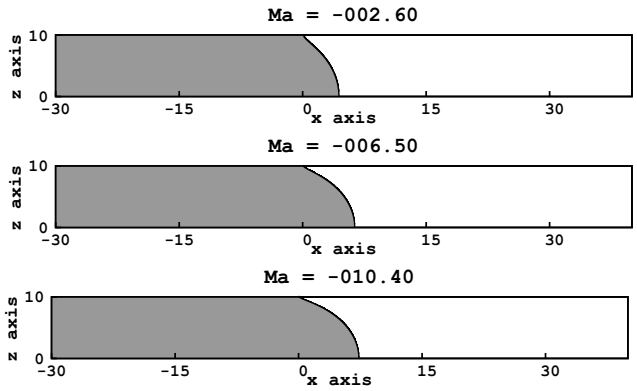

Fig. 3. Reaction fronts propagating in a fluid layer with surface tension gradients corresponding to negative Marangoni numbers. The front near the surface is pushed back due to fluid flow. We observe a larger distorsion for larger absolute values of the Marangoni number.

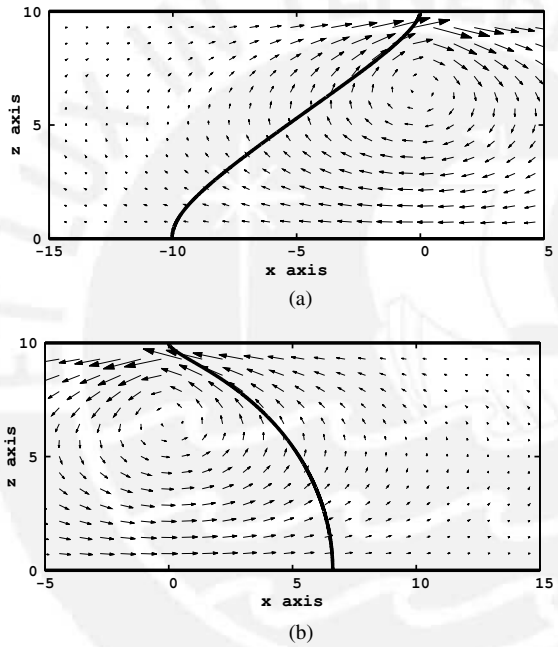

Fig. 4. Fluid flow induced by the surface tension gradient for (a) a positive Marangoni numbers (Ma=3.9) and (b) for a negative Marangoni number (Ma= −7.8).

appears with a larger distorsion. In the case of negative Marangoni numbers the situation is reversed as shown in Fig. 3. The leading portion of the front is located near the bottom of the container instead of the open surface. We also found that larger absolute values of the Marangoni number generate larger distance between tip and lagging portion. In Fig. 4 we show the velocity field acting near the reaction front. Surface tension gradients generate fluid motion near the open surface. The flow near the open surface is in the same direction of front propagation for positive Marangoni numbers, and in the opposite directions for negative Marangoni numbers. The flow takes the form of a single convective roll, with the flow moving in an opposite direction

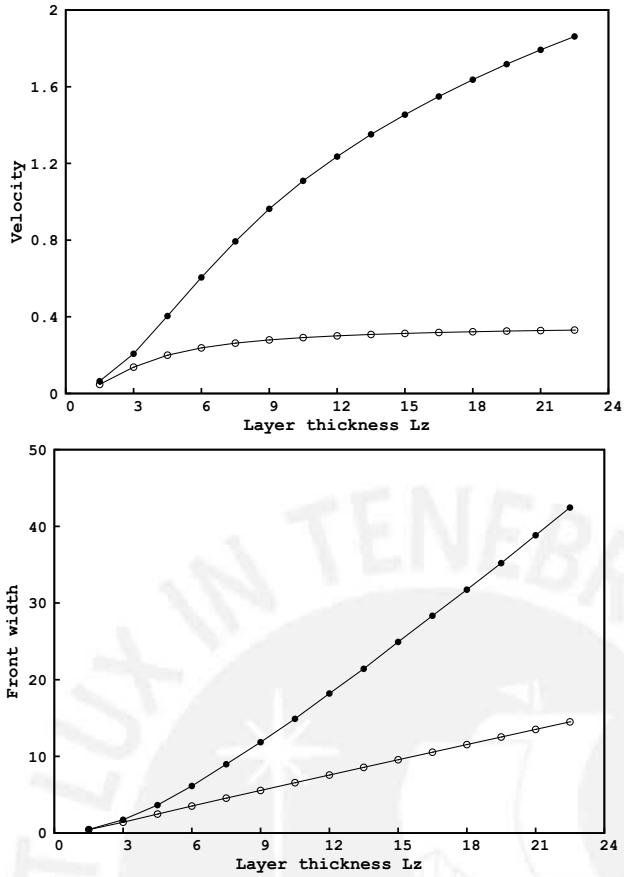

Fig. 5. Front speed and width as functions of layer thickness. The front speed (a) increases as the layer thickness increases for both Ma=6.5 (solid circles) and Ma= −6.5 (open circles).

near the container wall parallel to the open surface. The shape of the convective roll is determined by a surface tension discontinuity proportional to a delta function. It is therefore identical for two Marangoni numbers that have the same absolute value, but rotating in opposite directions if these numbers have opposite signs see Eq. (11). This flow increases the speed of all fronts, but it is higher for fronts that propagate in the same direction of the surface flow.

We analyzed the effects of the layer thickness in the speed and shape of the reaction fronts for a given Marangoni number. The speed of the front increases significantly for layer thicknesses shown in Fig. 5. The rate of increase slows down near $L_z = 22.5$, which is the upper limit of the range under study. This rate of increase corresponds to a larger distortion of the front as measured by the front width, defined as the distance between the leading front position and the lagging front position. These positions correspond to the maximum and minimum values of the front height fucntion $H(z,t)$ for a given time. The opposing directions of the fluid flow near the surface and near the container wall generates the distortion. As shown in Fig. 5b, the front width is higher for larger layer thickness. These trends are the same for positive and negative Marangoni numbers, in both cases the speed and thickness increase. However, for positive Marangoni numbers the increase is higher compared to the same Marangoni number but of opposite sign.

5 Summary and discussion

We showed that surface tension driven convection modifies the front speed and shape for thin fronts modeled by the KPZ equation. These results are comparable to results obtained using a reaction-diffusion model, in particular if the Marangoni number is small. This fact is consistent with the eikonal approximation of curved reaction-diffusion fronts, given that the deterministic KPZ equation is a small curvature approximation of the eikonal relation. Therefore we expect that our results apply to a large class of reaction-diffusion fronts where the eikonal relation is valid. These results include a larger increase of speed for positive Marangoni numbers, where the fluid flow near the surface is in the same direction as the direction of propagation of the front. Negative Marangoni numbers still increase the speed of the front, but not at the same rate as positive Marangoni numbers. For a constant Marangoni number, the front speed is higher if the layer thickness is larger. We also have that the front distorsion is larger for thicker layers. The comparison between these models was carried out using free boundary conditions everywhere, except in the surface where the surface tension gradient takes place. Results from the front propagation model will have to be tested with the appropriate boundary conditions. Qualitative aspects, such as the leading front tip in open containers, can be explained with the change of surface tension across the front. Detailed comparisons with current experiments in the iodate-arsenous acid reaction will require the inclusion of density driven convection [6]. The thin front model can be extended to treat this case.

This work was supported by a grant from the Dirección de Gestión de la Investigación (DGI 2014-0003) of the Pontificia Universidad Católica del Perú.

References

1. K. Matthiessen, H. Wilke, S.C. Muller, Phys. Rev. E. **53**, 6056 (1996)
2. H. Kitahata, R. Aihara, N. Magome, Kenichi Yoshikawa, J. Chem. Phys. **116**, 5666 (2002)
3. H. Kitahata, K. Yoshikawa, Physica D **205**, 283 (2005)
4. H. Miike, H. Yamamoto, S. Kai, Stefan C. Muller, Phys. Rev. E **48**, R1627(R) (1993)
5. E. Popity-Toth, V. Pimienta, D. Horvath, A. Toth, J. Chem. Phys. **139**, 164707 (2013)
6. E. Popity-Toth, G. Potari, I. Erdos, D. Horvath, A. Toth, J. Chem. Phys. **141**, 044719 (2014)
7. L. Rongy, A. De Wit, J. Chem. Phys. **124**, 164705 (2006)
8. L. Rongy, A. De Wit, J. Eng. Math. **59**, 221 (2007)
9. M.A. Budroni, L. Rongy, A. De Wit, Phys. Chem. Chem. Phys. **14**, 14619 (2012)
10. L. Rongy, P. Assemat, A. De Wit. Chaos, **22**, 037106 (2012)
11. J. Masere, D.A. Vasquez, B.F. Edwards, J.W. Wilder, K. Showalter, J. Phys. Chem. **98**, 6505 (1994)
12. J.W. Wilder, D.A. Vasquez, B.F. Edwards, Phys. Rev. E **56**, 3016 (1997)
13. D.A. Vasquez, E. Thoreson, Chaos **12**, 49 (2002)
14. J.J. Tyson, J.P. Keener, Physica D **32**, 327 (1988)
15. C.A.J. Fletcher, *Computational Techniques for Fluid Dynamics, 2nd ed.* (Springer-Verlag, New York, 1991)
16. J.W. Wilder, B.F. Edwards, D.A. Vasquez, G.I. Sivashinsky, Physica D **73**, 217 (1994)
17. W.H. Press, B.P. Flannery, S.A Teukolsky, W.T. Vetterling, *Numerical Recipes in FORTRAN: The Art of Scientific Computing, 2nd edn.* (Cambridge University Press, Cambridge, England, 1992)

Surface tension driven flow on a thin reaction front

R.Guzmán

PUCP

Indice

1. Introducción
   - Trabajos iniciales
   - Trabajos relacionados
2. Modelo bidimensional
   - Navier - Stokes
   - Reacción - Difusión
   - Solución numérica
   - Resultados
3. Modelo de frente químico
   - Ecuación KPZ
   - Resultados

Miike, Yamamoto (1993)

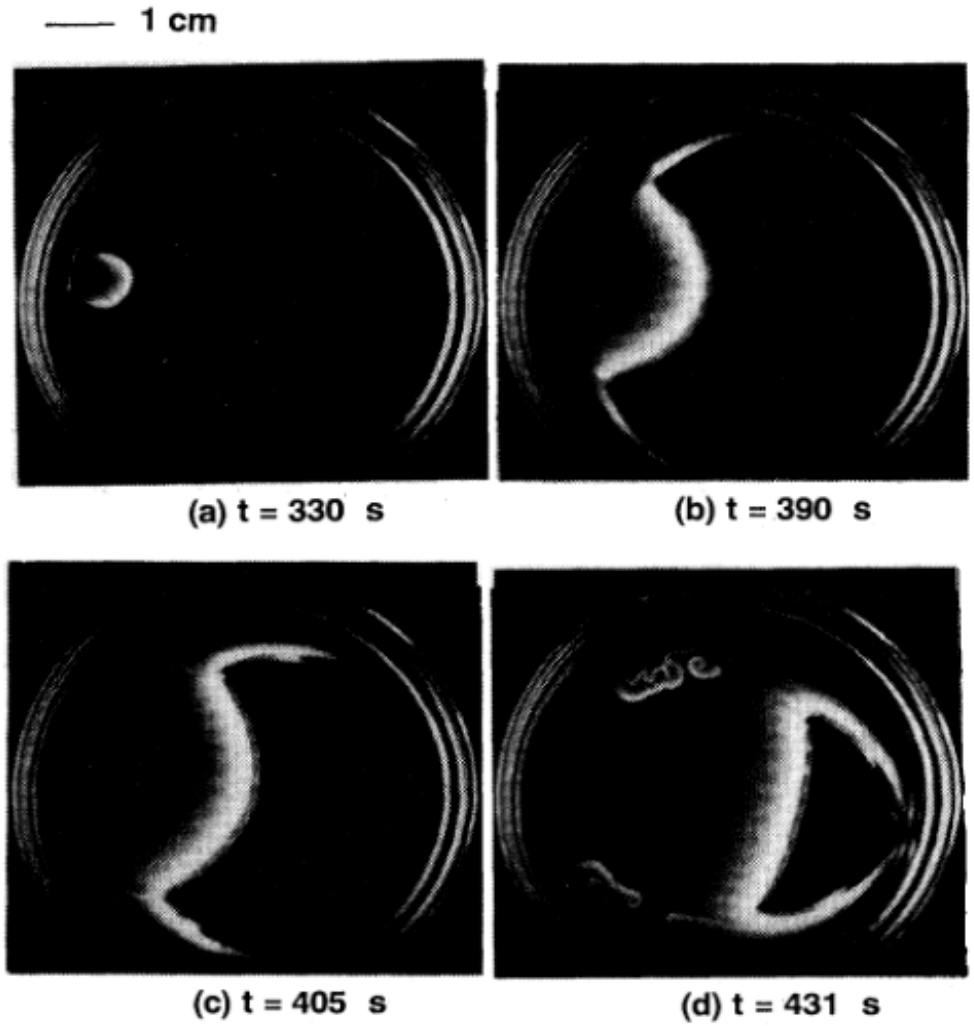

FIG. 1. Picture sequence showing front propagation of a "big wave," triggered by 10 s immersion of silver wire at trigger time $t_{tr} = 5$ min (after mixing the catalyst to the BZ regent).

Pópity, Pimienta, Horváth,Tóth (2013)

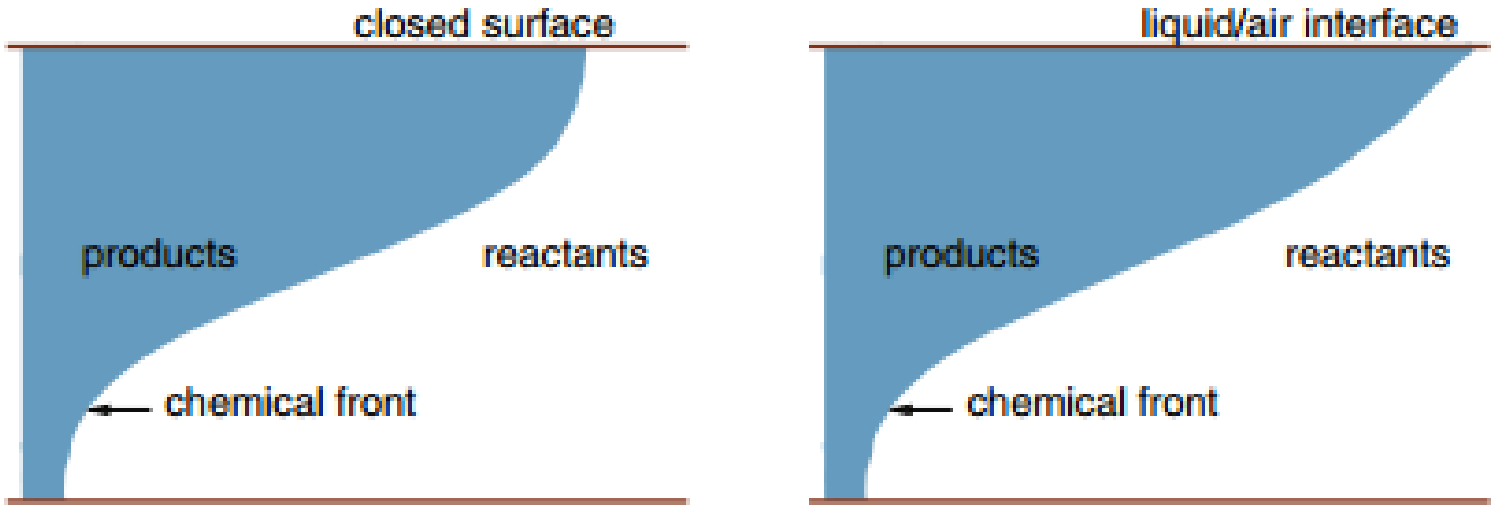

FIG. 1. Sketch of the system governed by a single convection roll. With closed surface on the top buoyancy drives the less dense product solution ahead on the top, tilting the reaction front (left). In the presence of open surface the gradient of surface tension generates additional flow on the top, further elongating the reaction front (right).

Pópity, Pótári, Erdös, et al. (2014)

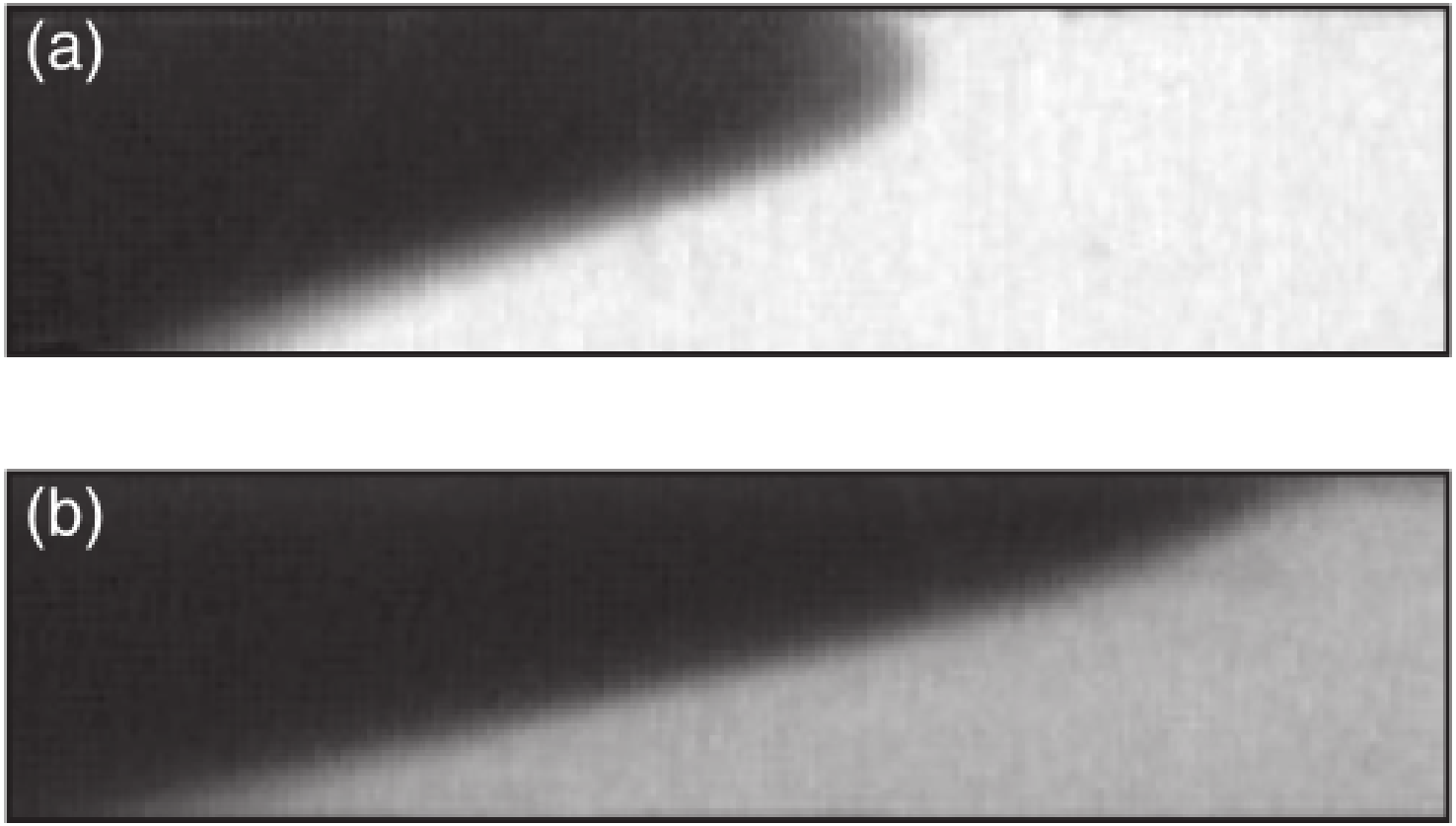

FIG. 2. Side view images of reaction fronts propagating from left to right in a reaction vessel with $L_y = 5$ mm: without free surface (a) and with free surface on top (b). The lighter region corresponds to the reactants and the darker region represents the product solution. Field view: 7.3 mm $\times$ 1.7 mm.

Rongy, De Wit (2006)

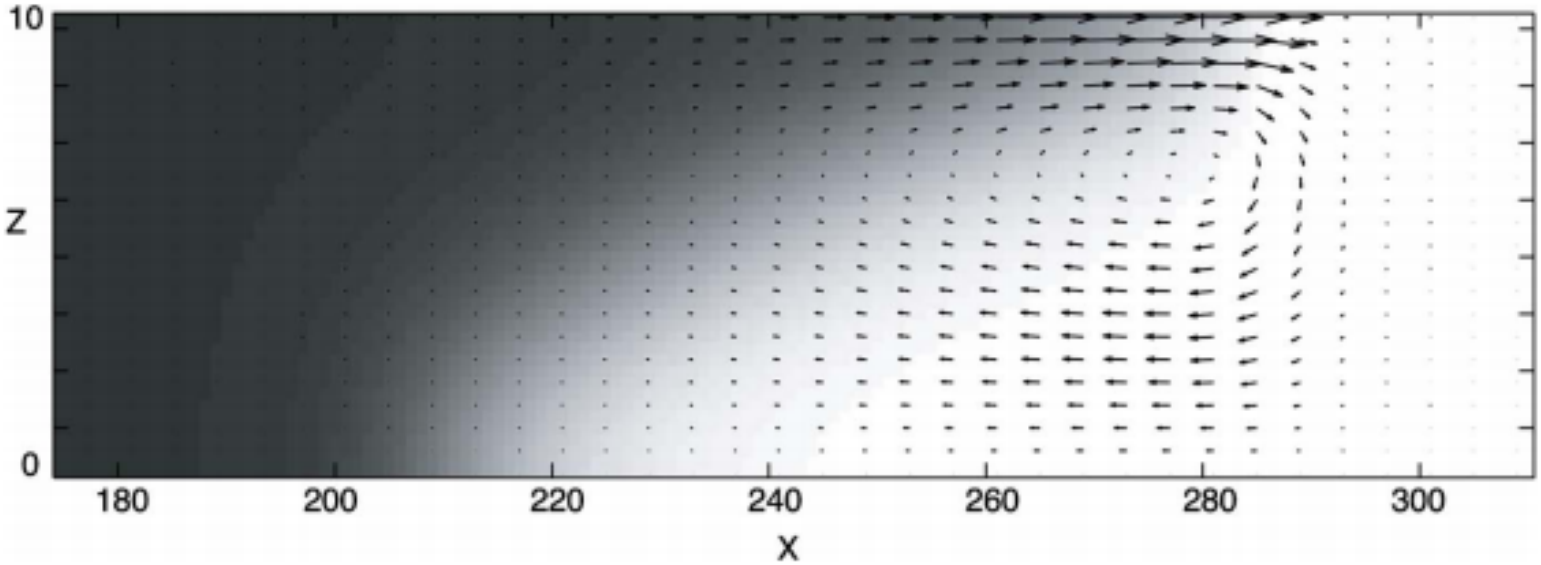

Edwards, Wilder, Showalter (1991)

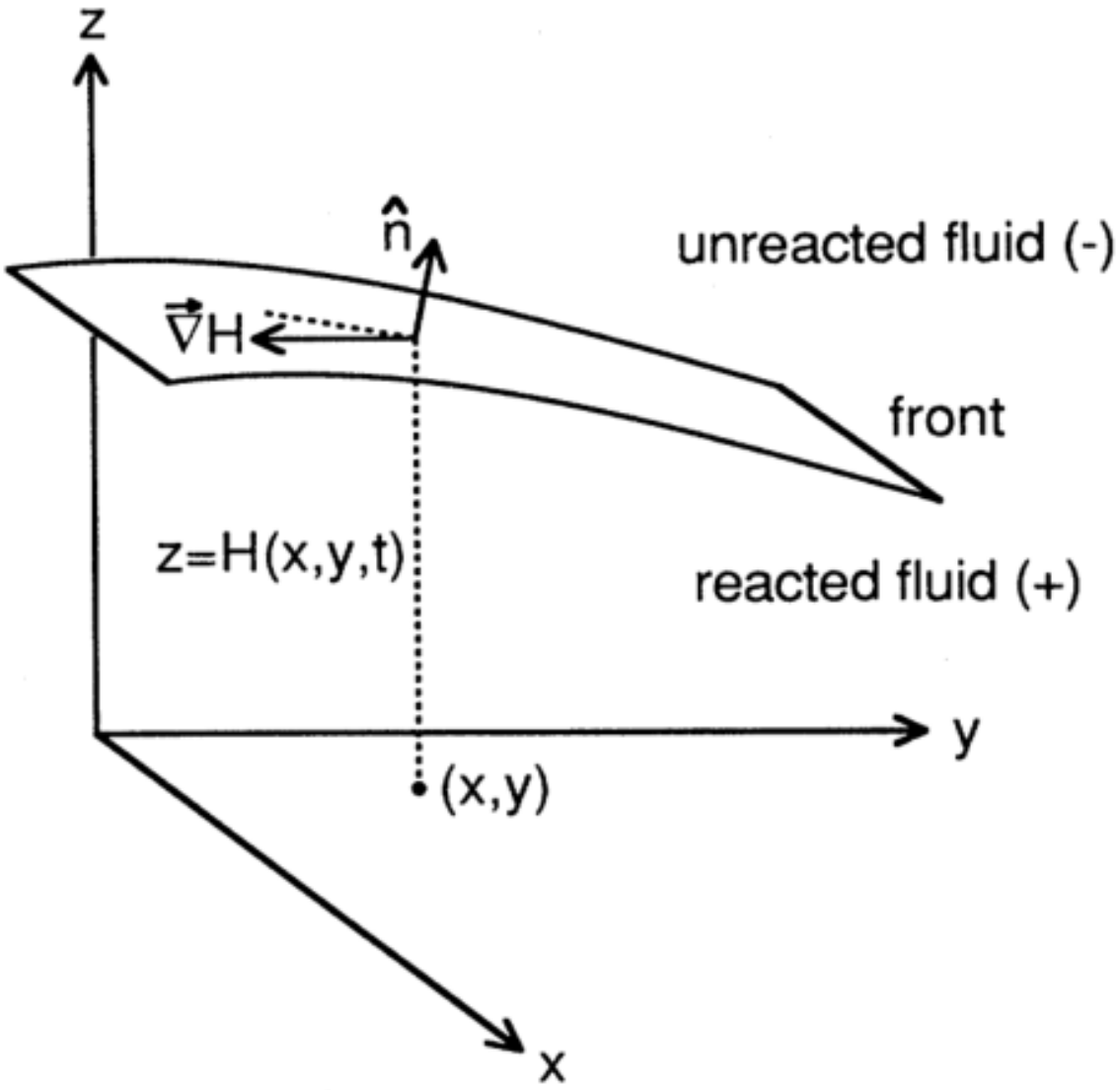

Wilder, Vásquez, Edwards (1997)

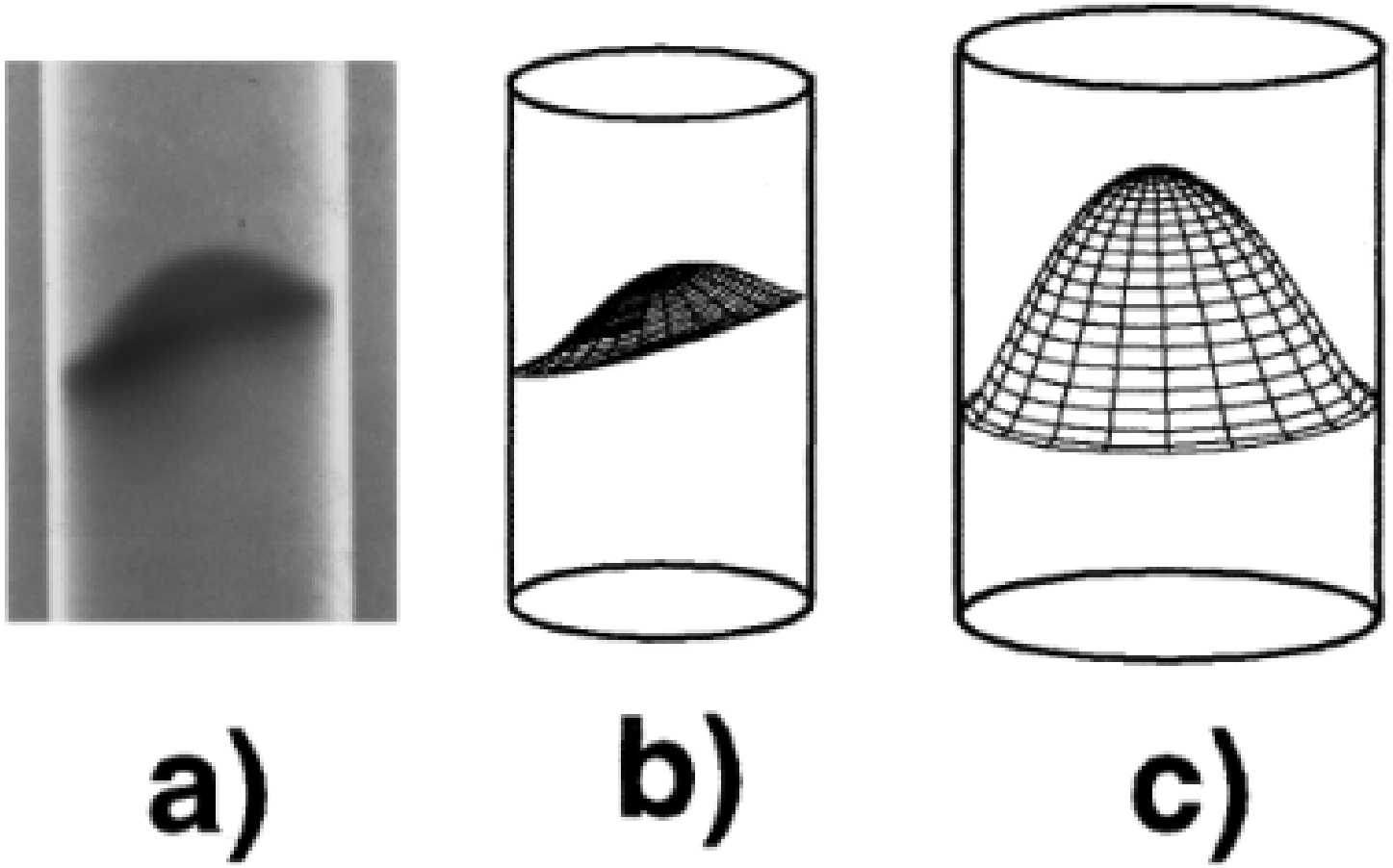

FIG. 2. Shown are an experimental front in a tube with diameter 0.16 cm (a), a computed front in a tube of diameter 0.16 cm (b), and a computed front in a tube of diameter 0.23 cm (c).

Navier - Stokes

Ecuacion de Navier-Stokes sin unidades:

$$\frac{\partial \boldsymbol{v}}{\partial t} + \boldsymbol{v} \cdot \nabla \boldsymbol{v} = S_c(-\nabla \mathcal{P} + \nabla^2 \boldsymbol{v})$$

$$L = \frac{D}{c_0}; t = \frac{D}{c_0^2}$$

Reacción - Difusión

Modelo de reacción autocatalítica: $A + 2C \rightarrow 3C$

$$\frac{\partial c}{\partial t} + \boldsymbol{v} \cdot \nabla c = \nabla^2 c + 2c^2(1-c)$$

Solución

Definimos: *Stream* (ψ) y *Vorticity* (ω)

Con lo que reducimos la ecuación de Navier-Stokes a:

$$\frac{\partial \omega}{\partial t} = \frac{\partial(\psi, \omega)}{\partial(x, z)} + S_c \nabla^2 \omega$$

Condiciones de frontera: número de Marangoni

$$\frac{\partial v_x}{\partial z} = -M \frac{\partial c}{\partial x}$$

$$M = -\frac{1}{\mu\sqrt{Dk}} \frac{\mathrm{d}\gamma}{\mathrm{d}c}$$

Resultados: M positivo

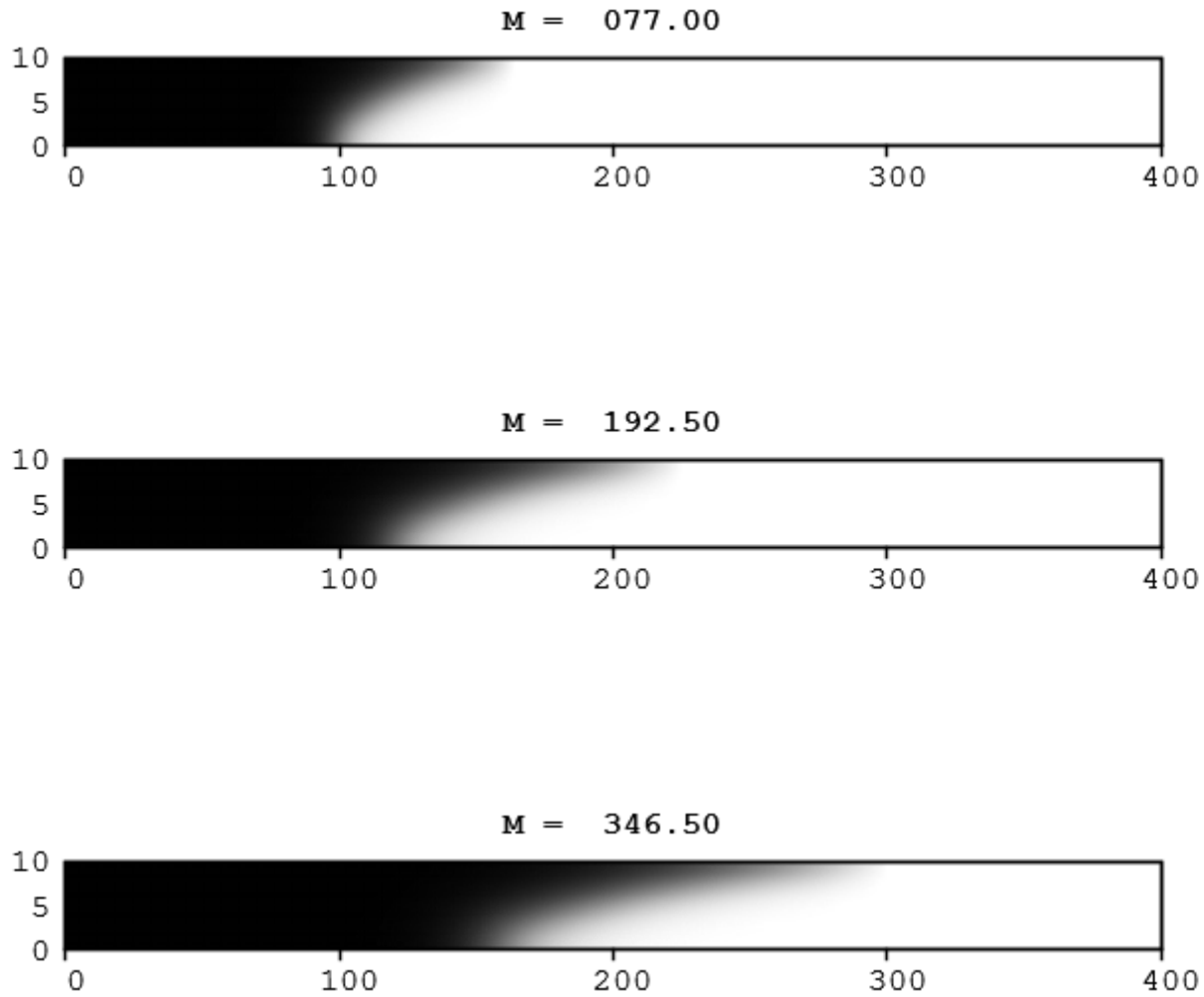

Resultados: M negativo

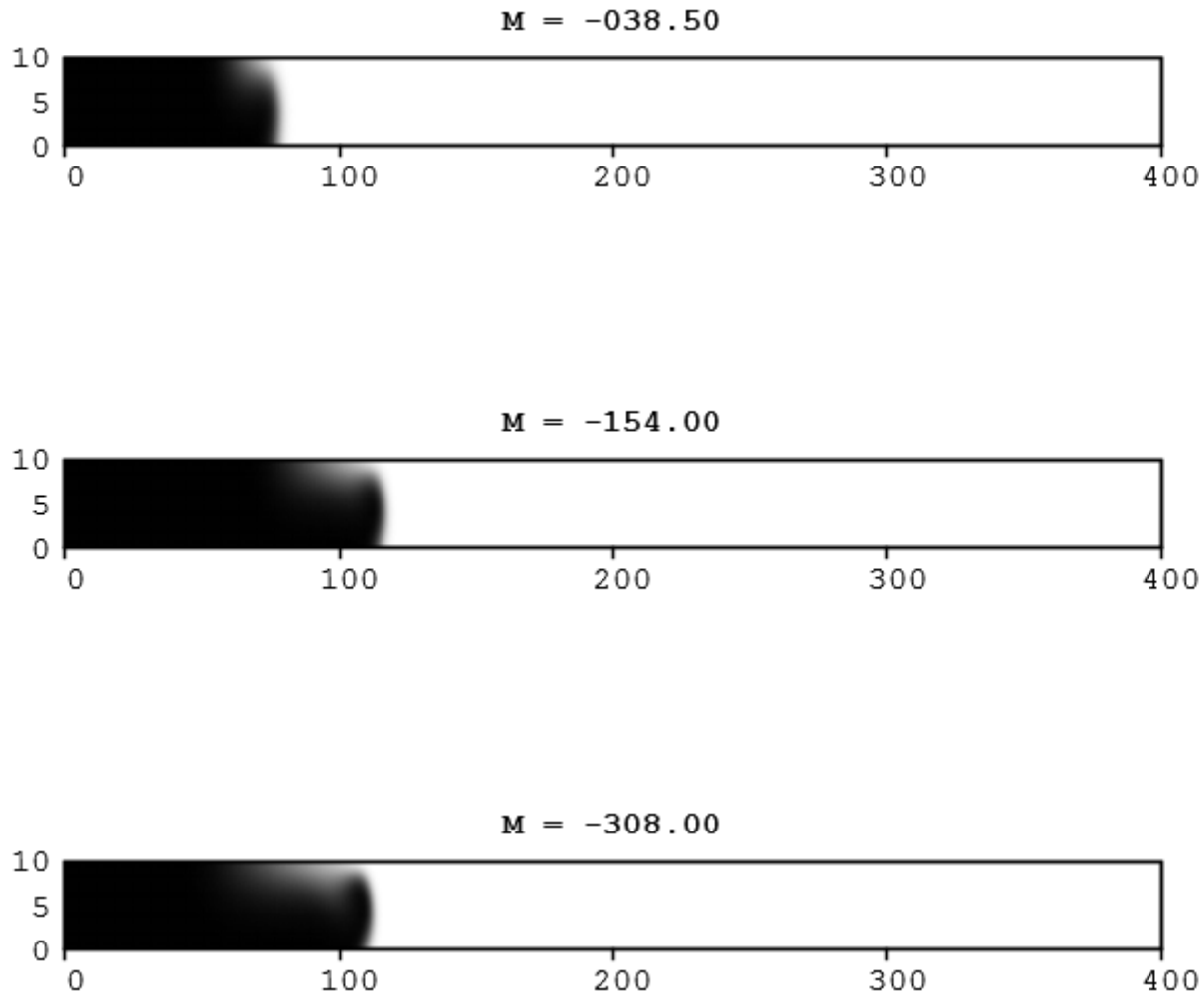

Resultado: velocidad de los frentes

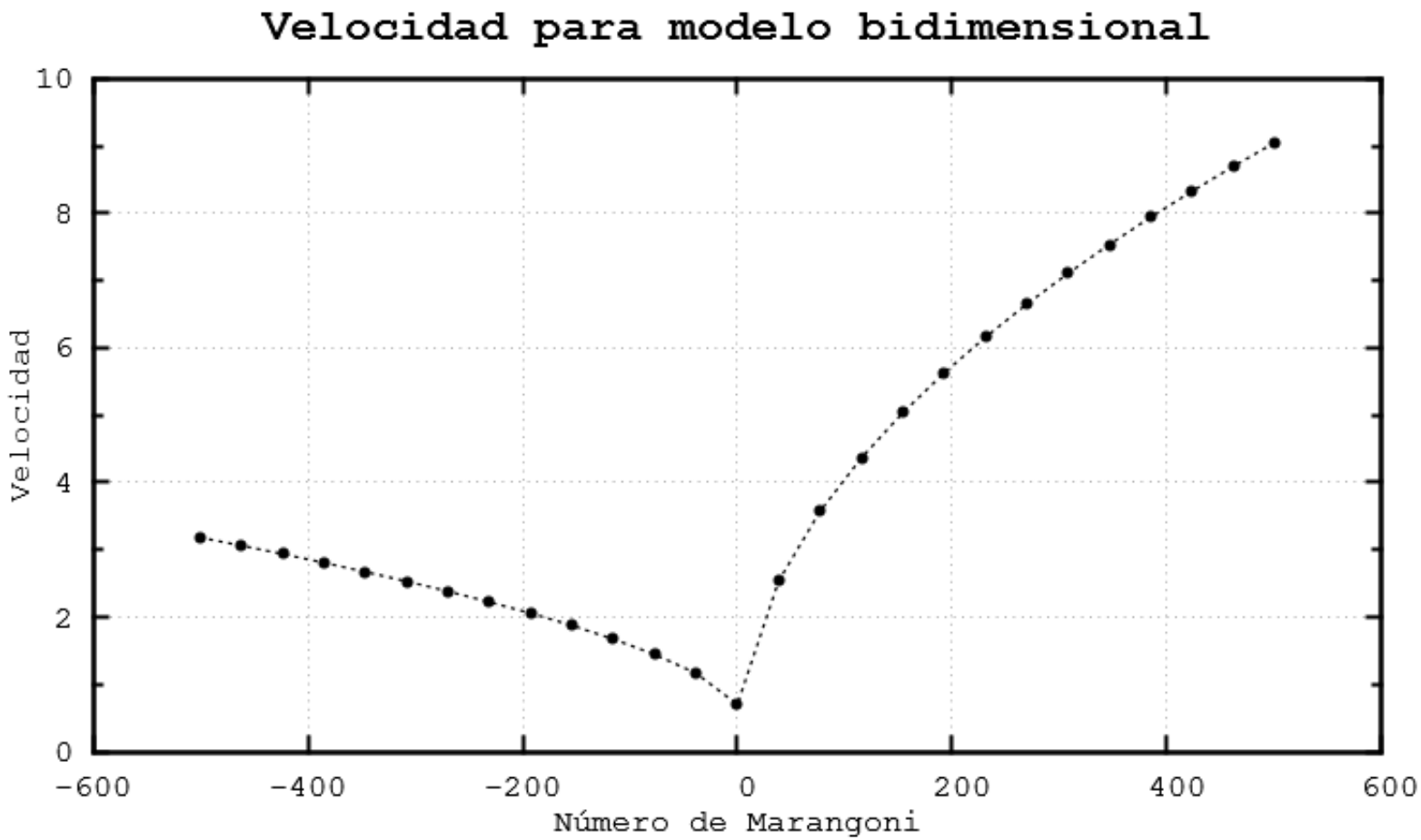

Ecuación KPZ

Para frentes delgados y de baja curvatura se tiene una ecuación KPZ para la evolución del frente:

$$\frac{\partial H}{\partial t} = \frac{C_0}{2}\left(\frac{\partial H}{\partial x}\right)^2 + D\frac{\partial^2 H}{\partial x^2} + \hat{\boldsymbol{n}} \cdot \vec{\boldsymbol{v}}$$

$$\omega(x,z) = -\frac{\mathrm{Ma}}{2L_z}\frac{\sin(\pi z/L_z)}{\cos(\pi z/L_z)+\cosh(\pi x/L_z)}$$

Resultados: ecuación KPZ

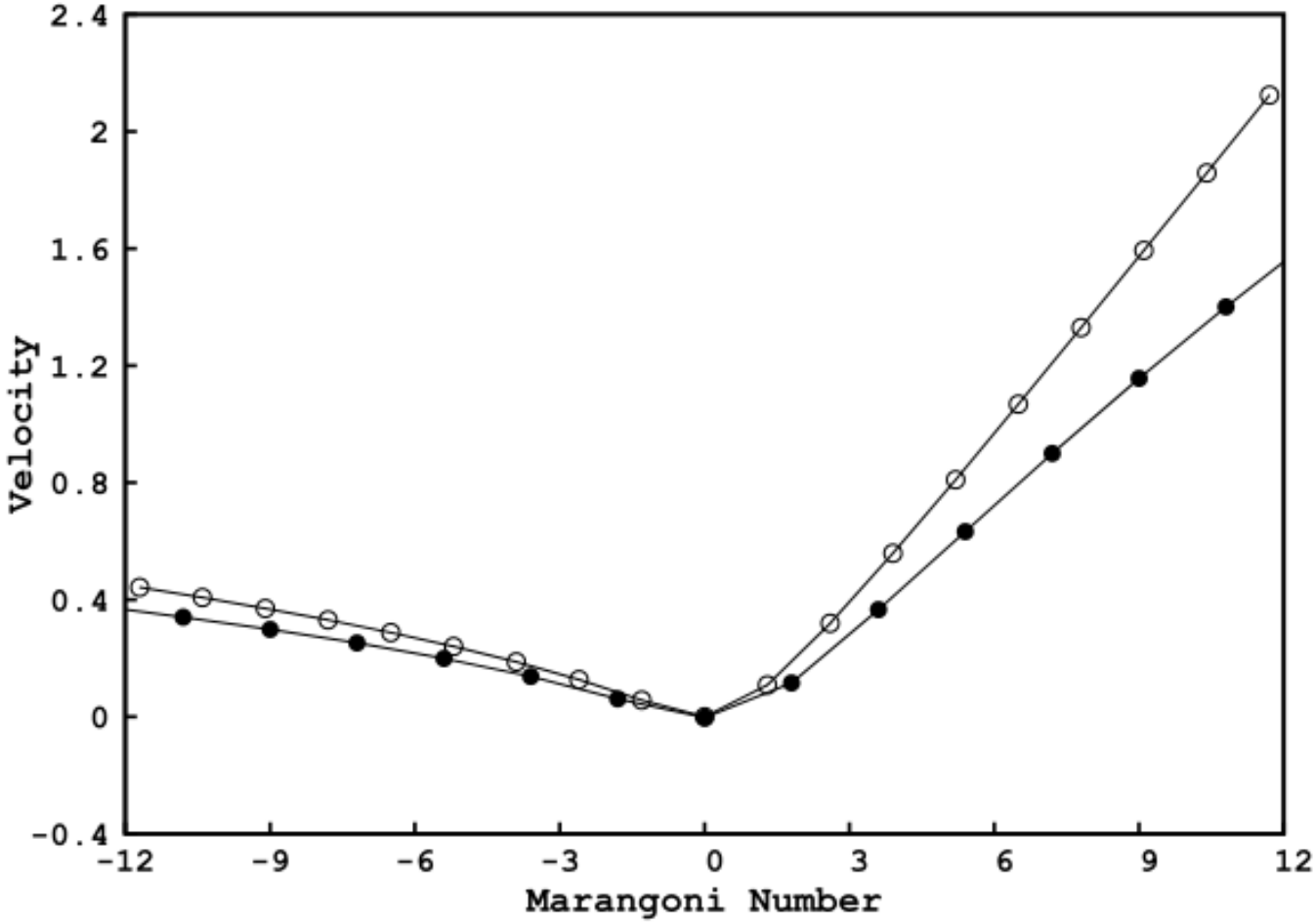

Fig. 1. The increase of front speed as a function of Marangoni number for fronts propagating on a layer of thickness $L_z = 10$. The open circles correspond to fronts described with the deterministic KPZ equation, while the solid circles are results using a reaction-diffusion equation. In both cases the speed of increase is enhanced by fluid flow.

Resultados: ecuación KPZ

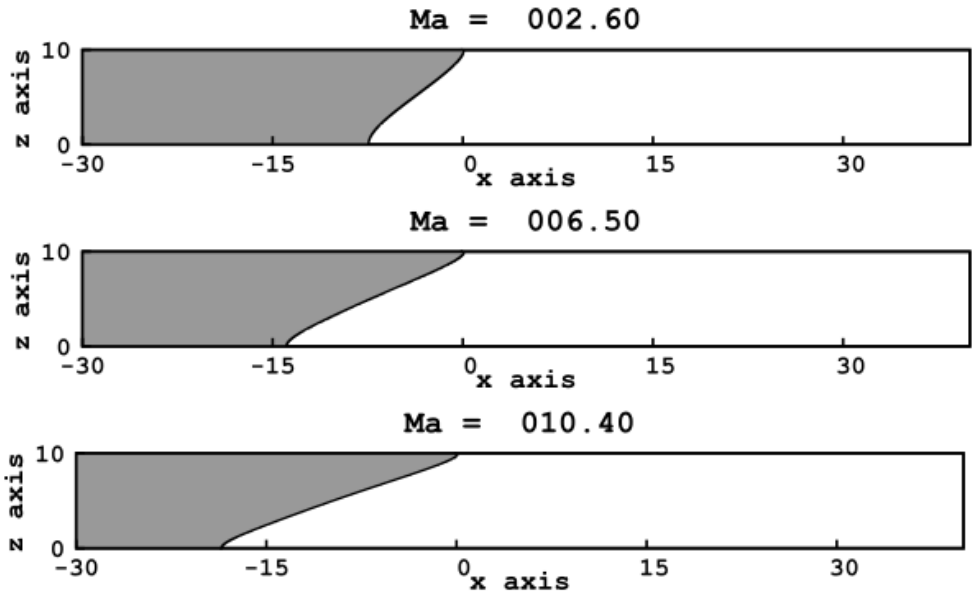

Fig. 2. Reaction fronts propagating in a fluid layer with surface tension gradients corresponding to positive Marangoni. The shape of the front develops a tip near the layer surface. The tip of the front is larger for larger Marangoni numbers.

Resultados: ecuación KPZ

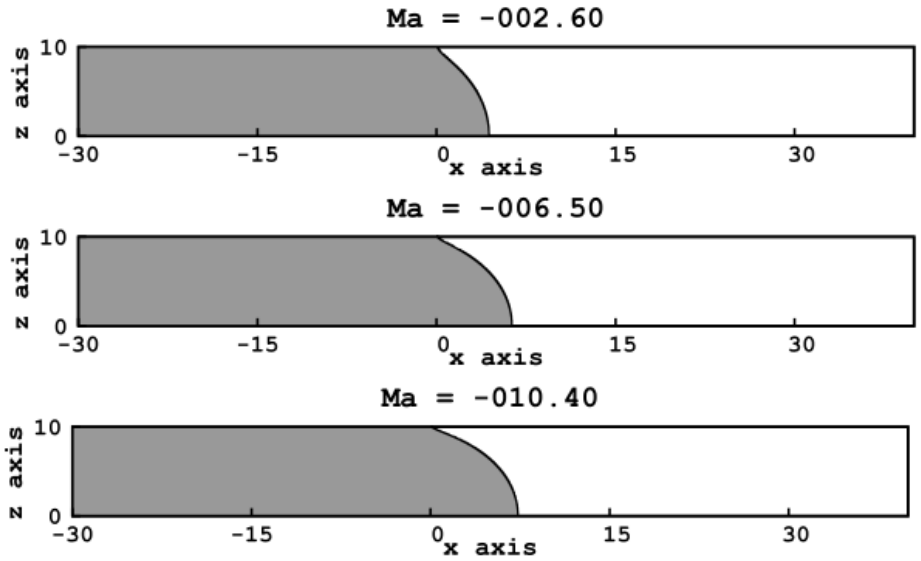

Fig. 3. Reaction fronts propagating in a fluid layer with surface tension gradients corresponding to negative Marangoni numbers. The front near the surface is pushed back due to fluid flow. We observe a larger distorsion for larger absolute values of the Marangoni number.

Resultados: ecuación KPZ

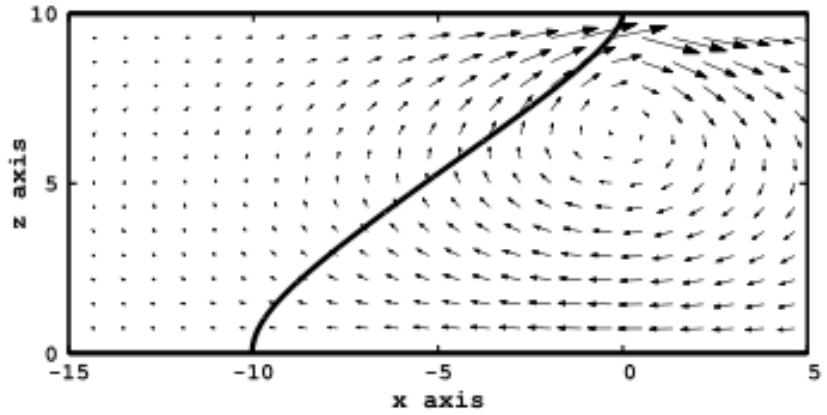

(a)

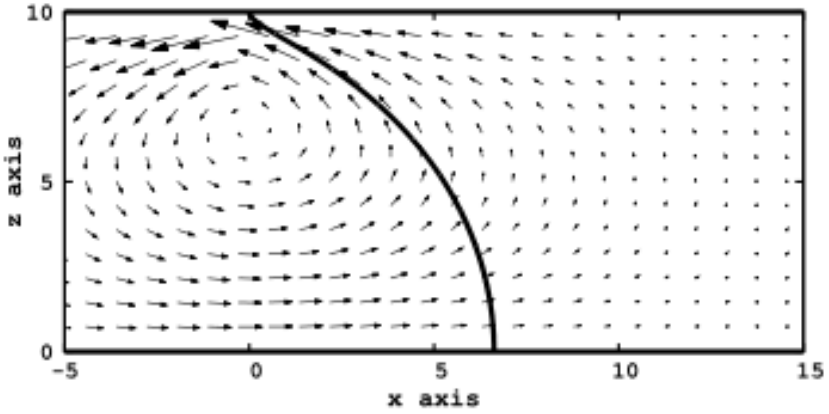

(b)

Fig. 4. Fluid flow induced by the surface tension gradient for (a) a positive Marangoni numbers (Ma=3.9) and (b) for a negative Marangoni number (Ma= −7.8).

Resultados: ecuación KPZ